PHYSICAL REVIEW D **88,** 101301(R) (2013)

Limits on anisotropic inflation from the Planck data

Jaiseung Kim*
Max-Planck-Institut für Astrophysik, Karl-Schwarzschild Strasse 1, 85741 Garching, Germany and Niels Bohr Institute, Blegdamsvej 17, DK-2100 Copenhagen, Denmark

Eiichiro Komatsu
Max-Planck-Institut für Astrophysik, Karl-Schwarzschild Strasse 1, 85741 Garching, Germany and Kavli Institute for the Physics and Mathematics of the Universe, Todai Institutes for Advanced Study, The University of Tokyo, Kashiwa 277-8583, Japan

(Received 6 October 2013; published 14 November 2013)

Temperature anisotropy of the cosmic microwave background offers a test of the fundamental symmetry of spacetime during cosmic inflation. Violation of rotational symmetry yields a distinct signature in the power spectrum of primordial fluctuations as $P(\mathbf{k}) = P_0(k)[1 + g_*(\hat{\mathbf{k}} \cdot \hat{\mathbf{E}}_{\rm cl})^2]$, where $\hat{\mathbf{E}}_{\rm cl}$ is a preferred direction in space and g_* is an amplitude. Using the Planck 2013 temperature maps, we find no evidence for violation of rotational symmetry, $g_* = 0.002 \pm 0.016$ (68% C.L.), once the known effects of asymmetry of the Planck beams and Galactic foreground emission are removed. (Based on observations obtained with the Planck Collaboration, a ESA science mission with instruments and contributions directly funded by ESA Member States, NASA, and Canada.)

DOI: 10.1103/PhysRevD.88.101301 PACS numbers: 98.70.Vc, 98.80.Cq, 98.80.Es

Cosmic inflation [1–5], an indispensable building block of the standard model of the Universe, is described by *nearly* de Sitter spacetime. The metric charted by flat coordinates is given by $ds^2 = -dt^2 + e^{2Ht}d\mathbf{x}^2$, where H is the expansion rate of the Universe during inflation. This spacetime admits ten isometries: three spatial translations, three spatial rotations, one time translation accompanied by spatial dilation ($t \to t - \lambda/H$ and $\mathbf{x} \to e^{\lambda}\mathbf{x}$ with a constant λ), and three additional isometries which reduce to special conformal transformations in $t \to \infty$. The necessary time dependence of the expansion rate $Ht \to \int H(t')dt'$ breaks the time translation symmetry hence the spatial dilation symmetry, yielding the two-point correlation function of primordial fluctuations that is nearly, but not exactly, invariant under $\mathbf{x} \to e^{\lambda}\mathbf{x}$ [6]. The magnitude of the deviation from dilation invariance is limited by that of the time dependence of H, i.e., $-\dot{H}/H^2 = \mathcal{O}(10^{-2})$.

In the usual model of inflation, six out of ten isometries remain unbroken: translations and rotations. Why must they remain unbroken while the others are broken? In this paper, we shall test rotational symmetry during inflation using the two-point correlation function of primordial perturbations to spatial curvature ζ generated during inflation. This is defined as a perturbation to the exponent in the spatial metric, $\int H(t')dt' \to \int H(t')dt' + \zeta(\mathbf{x}, t)$. In Fourier space, we write the two-point function as $\langle \zeta_{\mathbf{k}} \zeta^*_{\mathbf{k}'} \rangle = (2\pi)^3 \delta^{(3)}(\mathbf{k} - \mathbf{k}')P(\mathbf{k})$, and $P(\mathbf{k})$ is the power spectrum. Translation invariance, which is kept in this paper, gives the delta function, while rotation invariance, which is *not* kept, would give $P(\mathbf{k}) \to P(k)$ with $k \equiv |\mathbf{k}|$. Dilation invariance would give $k^3P(k) = \text{const}$, whereas a small deviation $k^3P(k) \propto k^{-0.04}$ has been detected from the cosmic microwave background (CMB) data with more than 5-σ significance [7,8].

Following Ref. [9], we write the power spectrum as $P(\mathbf{k}) = P_0(k)[1 + g_*(k)(\hat{\mathbf{k}} \cdot \hat{\mathbf{E}}_{\rm cl})^2]$, where $\hat{\mathbf{E}}_{\rm cl}$ is a preferred direction in space, g_* is a parameter characterizing the amplitude of violation of rotational symmetry, and $P_0(k)$ is an isotropic power spectrum which depends only on the magnitude of the wave number, k. This form is generic, as it is the leading-order anisotropic correction that remains invariant under parity flip, $\mathbf{k} \to -\mathbf{k}$. "Anisotropic inflation" models, in which a scalar field is coupled to a vector field (see Refs. [10–12] and references therein) can produce this form.[1] A very long-wavelength perturbation on superhorizon scales can also produce this form via a three-point function [17]. A preinflationary universe was probably chaotic and highly anisotropic, and thus a remnant of the preinflationary anisotropy may still be detectable [18].

We shall ignore a potential k dependence of g_* in this paper. We expand $g_*(\hat{\mathbf{k}} \cdot \hat{\mathbf{E}}_{\rm cl})^2$ using spherical harmonics:

$$g_*(\hat{\mathbf{k}} \cdot \hat{\mathbf{E}}_{\rm cl})^2 = \frac{g_*}{3} + \frac{8\pi}{15} g_* \sum_M Y^*_{2M}(\hat{\mathbf{E}}_{\rm cl}) Y_{2M}(\hat{\mathbf{k}}). \quad (1)$$

We then write the power spectrum as

*kim@mpa-garching.mpg.de

[1] Anisotropic inflation models produce three-point functions of ζ which also depend on g_* [13–15]. The Planck team uses this property to put model-dependent constraints on g_* from non-detection of primordial three-point functions [16].

$$P(\mathbf{k}) = \tilde{P}_0(k)\left[1 + \sum_M g_{2M} Y_{2M}(\hat{\mathbf{k}})\right], \tag{2}$$

where we have absorbed $g_*/3$ into the normalization of the isotropic part, $\tilde{P}_0(k) \equiv P_0(k)(1 + g_*/3)$, and defined $g_{2M} \equiv \frac{8\pi}{15}\frac{g_*}{1+g_*/3} Y^*_{2M}(\hat{\mathbf{E}}_{\rm cl})$ with g_{2M} for $M < 0$ given by $g_{2,-M} = (-1)^M g^*_{2,M}$.

There are five parameters to be determined from the data. We denote the parameter vector as $\mathbf{h} \equiv \{g_{20}, \mathrm{Re}[g_{21}], \mathrm{Im}[g_{21}], \mathrm{Re}[g_{22}], \mathrm{Im}[g_{22}]\}$. We search for $\mathbf{h}$ in the covariance matrix of the spherical harmonics coefficients of CMB temperature maps, $\mathcal{C}_{l_1 m_1, l_2 m_2} \equiv \langle a_{l_1 m_1} a^*_{l_2 m_2}\rangle$, where $a_{lm} = \int d^2\hat{\mathbf{n}} T(\hat{\mathbf{n}}) Y^*_{lm}(\hat{\mathbf{n}})$. The anisotropic power spectrum of Eq. (2) gives [19]

$$\mathcal{C}_{l_1 m_1, l_2 m_2} = \delta_{l_1 l_2}\delta_{m_1 m_2} C_{l_1} + \imath^{l_1 - l_2}(-1)^{m_1} D_{l_1 l_2} \times \sum_M g_{2M}\left[\frac{5(2l_1+1)(2l_2+1)}{2\pi}\right]^{\frac{1}{2}} \begin{pmatrix} 2 & l_1 & l_2 \\ 0 & 0 & 0 \end{pmatrix} \times \begin{pmatrix} 2 & l_1 & l_2 \\ M & -m_1 & m_2 \end{pmatrix}, \tag{3}$$

where the matrices denote the Wigner 3-j symbols, and $D_{l_1 l_2} \equiv \frac{2}{\pi}\int k^2 dk \tilde{P}_0(k) g_{Tl_1}(k) g_{Tl_2}(k)$ with $g_{Tl}(k)$ the temperature radiation transfer function.

In the limit of weak anisotropy, the likelihood of the CMB data given a model may be expanded as

$$\mathcal{L} = \mathcal{L}|_{h=0} + \sum_i \frac{\partial \mathcal{L}}{\partial h_i}\bigg|_{h=0} h_i + \sum_{ij}\frac{1}{2}\frac{\partial^2 \mathcal{L}}{\partial h_i \partial h_j}\bigg|_{h=0} h_i h_j + \mathcal{O}(h^3). \tag{4}$$

The first and second derivatives are given by

$$\frac{\partial \mathcal{L}}{\partial h_i} = \mathcal{H}_i - \langle \mathcal{H}_i \rangle, \tag{5}$$

$$\frac{\partial^2 \mathcal{L}}{\partial h_i \partial h_j} = -\frac{1}{2}\,\mathrm{Tr}\left[\mathbf{C}^{-1}\frac{\partial \mathbf{C}}{\partial h_i}\mathbf{C}^{-1}\frac{\partial \mathbf{C}}{\partial h_j}\right], \tag{6}$$

where $\mathcal{H}_i \equiv \frac{1}{2}[\mathbf{C^{-1}}\boldsymbol{a}]^\dagger \frac{\partial \mathbf{C}}{\partial h_i}[\mathbf{C^{-1}}\boldsymbol{a}]$, and $\boldsymbol{a}$ denotes a_{lm} measured from the data and $\mathbf{C} \equiv \langle \boldsymbol{a}\boldsymbol{a}^\dagger\rangle$, both of which include noise and the other data-specific terms.

We obtain an estimator for $\mathbf{h}$ by maximizing the likelihood with respect to $\mathbf{h}$ [20]

$$\hat{h}_i = \sum_j [\mathcal{F}^{-1}]_{ij}(\mathcal{H}_j - \langle \mathcal{H}_j \rangle), \tag{7}$$

$$\mathcal{F}_{ij} \equiv \frac{1}{2}\,\mathrm{Tr}\left[\mathbf{C}^{-1}\frac{\partial \mathbf{C}}{\partial h_i}\mathbf{C}^{-1}\frac{\partial \mathbf{C}}{\partial h_j}\right]. \tag{8}$$

The covariance matrix $\mathbf{C}$ is neither diagonal in pixel nor harmonic space. In order to reduce the computational cost, we shall approximate it as diagonal in harmonic space. While this approximation makes our estimator suboptimal, it remains unbiased. The new estimator is

$$\hat{h}_i = \frac{1}{2}\sum_j (\mathbf{F}^{-1})_{ij} \sum_{l_1 m_1}\sum_{l_2 m_2}\frac{\partial \mathcal{C}_{l_1 m 1, l_2 m_2}}{\partial h_j} \times \frac{\tilde{a}^*_{l_1 m_1}\tilde{a}_{l_2 m_2} - \langle \tilde{a}^*_{l_1 m_1}\tilde{a}_{l_2 m_2}\rangle_{h=0}}{(C_{l_1} + N_{l_1})(C_{l_2} + N_{l_2})}, \tag{9}$$

where $\tilde{a}_{lm} \equiv \int d^2\hat{\mathbf{n}} T(\hat{\mathbf{n}}) M(\hat{\mathbf{n}}) Y^*_{lm}(\hat{\mathbf{n}})$ is the spherical harmonic coefficients computed from a masked temperature map [$M(\hat{\mathbf{n}}) = 0$ in the masked pixels, and 1 otherwise], and C_l and N_l are the signal and noise power spectra, respectively. The matrix $\mathbf{F}$ is defined by

$$F_{ij} \equiv \frac{f^2_{\rm sky}}{2}\sum_{l_1 m_1}\sum_{l_2 m_2}\frac{1}{C_{l_1} + N_{l_1}}\frac{\partial \mathcal{C}_{l_1 m 1, l_2 m_2}}{\partial h_i}\frac{1}{C_{l_2} + N_{l_2}} \times \frac{\partial \mathcal{C}_{l_1 m 1, l_2 m_2}}{\partial h_j}, \tag{10}$$

with $f_{\rm sky} \equiv \int \frac{d^2\hat{\mathbf{n}}}{4\pi} M(\hat{\mathbf{n}})$ the fraction of unmasked pixels.

Here, $\langle \tilde{a}^*_{l_1 m_1}\tilde{a}_{l_2 m_2}\rangle_{h=0}$ in Eq. (9) is the "mean field," which is nonzero even when $g_* = 0$. Data-specific issues such as an incomplete sky coverage, inhomogeneous noise, and asymmetric beams generate the mean field.

As we estimate $\hat{\mathbf{h}}$ by summing over many pairs of coefficients a_{lm}, we expect it to follow a Gaussian distribution (the central limit theorem). The likelihood of $\mathbf{h} \equiv \{g_{20}, \mathrm{Re}[g_{21}], \mathrm{Im}[g_{21}], \mathrm{Re}[g_{22}], \mathrm{Im}[g_{22}]\}$ is

$$\mathcal{L} = \frac{1}{|(2\pi)\mathbf{G}|^{1/2}}\exp\left\{-\frac{1}{2}[\hat{\mathbf{h}} - \mathbf{h}(g_*, \hat{\mathbf{E}}_{\rm cl})]^T \mathbf{G}^{-1} \times [\hat{\mathbf{h}} - \mathbf{h}(g_*, \hat{\mathbf{E}}_{\rm cl})]\right\}, \tag{11}$$

where $\mathbf{G}$ is the covariance matrix of $\hat{\mathbf{h}}$, which we estimate from Monte Carlo realizations. We compute the posterior distribution of g_* and $\hat{\mathbf{E}}_{\rm cl}$ by evaluating Eq. (11) using the Markov Chain Monte Carlo sampling [21].[2]

We use the Planck 2013 temperature maps at $N_{\rm side} = 2048$, which are available at the Planck Legacy Archive [23–25]. (We upgrade the low-frequency maps, which are originally at $N_{\rm side} = 1024$, to $N_{\rm side} = 2048$.) We use the map at 143 GHz as the main "CMB channel" and use the other frequencies as "foreground templates." We reduce the diffuse Galactic foreground emission by fitting templates to, and removing them from, the 143 GHz map. This

[2]One can calculate the expected error bars on g_{2M} using the Fisher matrix [22]. While such simplified calculations predict the same error bars on all components of g_{2M}, the actual error bars depend on M due to the shape of the mask. Also, the Fisher calculations assume homogeneous noise. Nonetheless, our error bars on g_{2M} from Monte Carlo simulations and our own Fisher calculations assuming homogeneous noise and the sky fraction of 71% are in agreement, to within 20%.

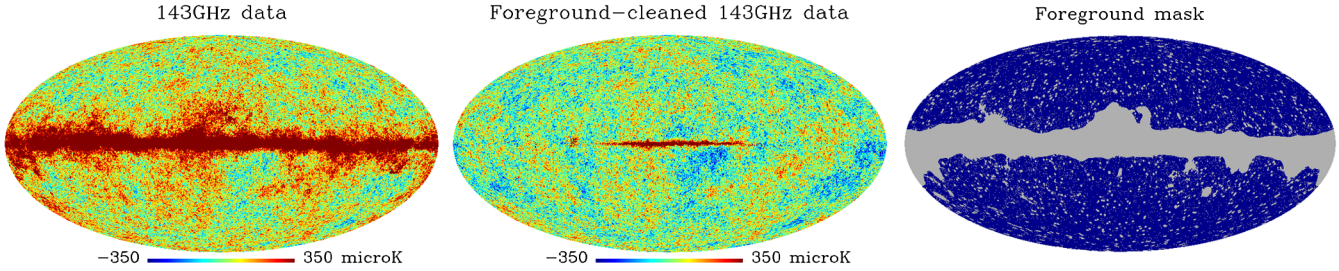

FIG. 1 (color online). (Left) The Planck temperature map at 143 GHz. (Middle) The foreground-reduced map at 143 GHz. (Right) The foreground mask. The maps are shown in a Mollweide projection in Galactic coordinates.

is similar to the method called SEVEM by the Planck Collaboration [26]. We derive the templates by taking a difference between two maps at neighboring frequencies. This procedure ensures the absence of CMB in the derived templates, producing five templates: $(30-44)$, $(44-70)$, $(353-217)$, $(545-353)$, and $(857-545)$ [GHz]. To create these difference maps, we first smooth a pair of maps to the common resolution. We smooth the low-frequency maps at 30–70 GHz as $a_{lm}^{(\nu)} \to a_{lm}^{(\nu)} b_l^G / b_l^{(\nu)}$, where $b_l^{(\nu)}$ is the beam transfer function at a frequency ν [27] and b_l^G is a Gaussian beam of $33'$ (FWHM). We smooth the high-frequency maps at 217–857 GHz as $a_{lm}^{(\nu)} \to a_{lm}^{(\nu)} b_l^{(143)} / b_l^{(\nu)}$, where $b_l^{(143)}$ is the beam transfer function at 143 GHz [28].

After the smoothing, we mask the locations of point sources and the brightest region near the Galactic center (3% of the sky) following SEVEM [26]. As the smoothed sources occupy more pixels, we enlarge the original point-source mask as follows: we create a map having 1 at the source locations and 0 otherwise, and smooth it. We then mask the pixels whose values exceed e^{-2}. We fit the templates to the 143 GHz map on the unmasked pixels (86% of the sky).

The left and middle panels of Fig. 1 show the original and foreground-reduced maps at 143 GHz, respectively. We still find significant foreground emission on the Galactic plane. We thus mask the regions contaminated by the residual foreground emission, combining the masks of various foreground-reduced maps produced by the Planck Collaboration (NILC, RULER, SEVEM, and SMICA [26]), and the point-source mask. We show the combined mask in the right panel of Fig. 1, which leaves 71% of the sky unmasked, and is similar to the "union mask" of the Planck Collaboration, except for a slightly enlarged point-source mask due to smoothing.

We use Eqs. (9) and (11) to compute g_{LM} from the masked foreground-reduced map. We restrict our analysis to the multipole range of $2 \le \ell \le 2000$. We compute the mean field from 1000 Monte Carlo realizations of signal and noise. The signal map is $T_S(\hat{\mathbf{n}}) = \sum_{lm} \sqrt{C_l}\, x_{lm} b_l^{(\nu)} p_l Y_{lm}(\hat{\mathbf{n}})$, where C_l is the best-fit "Planck + WP" power spectrum [8], p_l the pixel window function, and x_{lm} a Gaussian random variable with unit variance. The noise map is $T_N(\hat{\mathbf{n}}) = \sqrt{N(\hat{\mathbf{n}})} y(\hat{\mathbf{n}})$, where $N(\hat{\mathbf{n}})$ is the noise variance map provided by the Planck collaboration, and $y(\hat{\mathbf{n}})$ a Gaussian random variable with unit variance. We create high-frequency maps at $N_{\rm side} = 2048$, while we create low-frequency maps at $N_{\rm side} = 1024$ and upgrade to $N_{\rm side} = 2048$. We also compute g_{LM} from the signal-plus-noise simulations, and compute the covariance matrix, $\mathbf{G}$, in Eq. (11). Finally, we compute the posterior distribution of g_* and $\hat{\mathbf{E}}_{\rm cl}$ by evaluating Eq. (11) using the COSMOMC sampler [21].

The left panel of Fig. 2 shows the log-likelihood of locations of a preferred direction, $\ln \mathcal{L}(\hat{\mathbf{E}}_{\rm cl})$, given the Planck data. We find a significant detection of

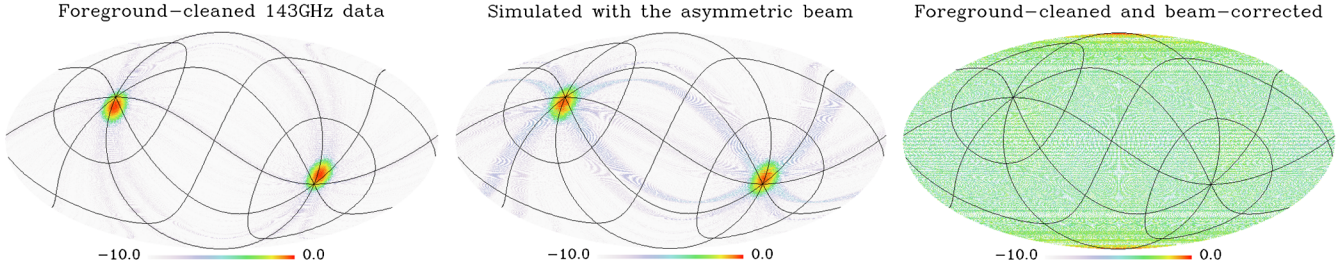

FIG. 2 (color online). (Left) Log-likelihood of locations of a preferred direction $\ln \mathcal{L}(\hat{\mathbf{E}}_{\rm cl})$ computed from the foreground-reduced map at 143 GHz. (Middle) $\ln \mathcal{L}(\hat{\mathbf{E}}_{\rm cl})$ from the average of simulations with the asymmetric beam. There are two peaks due to parity symmetry. The peaks lie close to the ecliptic pole. The overlaid grids show ecliptic coordinates. (Right) $\ln \mathcal{L}(\hat{\mathbf{E}}_{\rm cl})$ after removing the mean field due to the asymmetric beam. No obvious peaks are left.

$g_* = -0.111 \pm 0.013$ (68% C.L.) with $\hat{\mathbf{E}}_{\rm cl}$ pointing to $(l, b) = (94°.0^{+3°.9}_{-4°.0}, 23°.3 \pm 4°.1)$ in Galactic coordinates. This direction lies close to the ecliptic pole at $(l, b) = (96°.4, 29°.8)$.

This is essentially the same result as found from the WMAP data. Following the first detection reported in Ref. [29], the subsequent analysis finds $g_* = 0.29 \pm 0.031$ with $(l, b) = (94°, 26°) \pm 4°$ from the WMAP 5-year map at 94 GHz in the multipole range of $2 \le \ell \le 400$ [30] (also see [20]). They find a negative value at 41 GHz, $g_* = -0.18 \pm 0.04$. These signals, however, have been explained entirely by the effect of WMAP's asymmetric beams coupled with the scan pattern [31,32]. To confirm their results, we use the foreground-reduced WMAP 9-year maps [32], finding $g_* = -0.484^{+0.021}_{-0.023}$, $0.105^{+0.036}_{-0.028}$, and $0.355^{+0.038}_{-0.037}$ at 41, 61, and 94 GHz, respectively, in the multipole range of $2 \le \ell \le 1000$. The directions lie close to the ecliptic pole.

We find $g_* < 0$ from the Planck 143 GHz map. This is because the orientations of the semimajor axes of 143 GHz beams are nearly parallel to Planck's scan direction [28], which lies approximately along the ecliptic longitudes. As the beams are fatter along the ecliptic longitudes, the Planck measures less power along the ecliptic north-south direction than the east-west direction, yielding a quadrupolar power modulation with $g_* < 0$.[3]

We quantify and remove the effect of beam asymmetry by computing g_{LM} from 1000 signal-plus-noise simulations, in which the signal is convolved with Planck's asymmetric beams and scans. We have used the EFFCONV code, which was developed by the Planck Collaboration and publicly available[4] with the Planck effective beam data files [28,34]. The middle panel of Fig. 2 shows $\ln \mathcal{L}(\hat{\mathbf{E}}_{\rm cl})$ given the simulation data. We reproduce what we find from the real data: $g_* = -0.101 \pm 0.0004$ with $(96°.1 \pm 0°.1, 25°.9 \pm 0°.1)$ (the error bars are for the average of simulations). Using this result as the mean field [i.e., $\langle \tilde{a}^*_{l_1 m_1} \tilde{a}_{l_2 m_2} \rangle_{h=0}$ in Eq. (9)], we recompute $\ln \mathcal{L}(g_*, \hat{\mathbf{E}}_{\rm cl})$, finding no evidence for g_* (see also the right panel of Fig. 2, which shows no preferred direction). Our best limit is $g_* = 0.002 \pm 0.016$ (68% C.L.).

We have also analyzed the foreground-reduced 100 GHz map, which has less foreground emission than the 143 GHz map. We find 28- and 7-σ detections of g_* in the ecliptic-pole directions before and after the beam asymmetry correction, respectively. The 100 GHz beam is much less symmetric than the 143 GHz one [28]; thus, the beam simulation needs to be more precise for removing the asymmetry to the sufficient level. We find $g_* = -0.308 \pm 0.011$ before the beam asymmetry correction, which is consistent with the 100 GHz beams being more elongated along Planck's scan direction.

TABLE I. Best-fit amplitudes and directions with the 68% C.L. intervals. "BC" and "FR" stand for "beam correction" and "foreground reduction," respectively. The last row shows the result from the average of 1000 asymmetric beam simulations.

BC	FR	g_*	Direction (l, b) [degrees]
No	No	0.340 ± 0.018	$(226.6^{+21.2}_{-24.3}, 85.8 \pm 1.5)$
Yes	No	0.328 ± 0.018	$(141.1^{+18.6}_{-19.7}, 85.3 \pm 1.8)$
No	Yes	-0.111 ± 0.013	$(94.0^{+3.9}_{-4.0}, 23.3 \pm 4.1)$
Yes	**Yes**	$\mathbf{0.002 \pm 0.016}$	$(\mathbf{180.7^{+179.3}_{-180.7}}, \mathbf{44.8^{+45.2}_{-44.8}})$
No	...	-0.101 ± 0.0004	$(96.1 \pm 0.1, 25.9 \pm 0.1)$

Finally, we study the effect of Galactic foreground emission. Using the *raw* 143 GHz without cleaning, we find significant anisotropy: $g_* = 0.340$ and 0.328 ± 0.018 before and after the beam asymmetry correction, respectively. The directions lie close to the Galactic pole; thus, the foreground reduction plays an important role in nulling artificial anisotropy in the data.

We summarize our finding in Table I. After removing the effects of Planck's asymmetric beams and Galactic foreground emission, we find no evidence for g_*. Our limit, about 2% in g_*, provides the most stringent test of rotational symmetry during inflation.

J. K. would like to thank Belen Barreiro, Carlo Baccigalupi, Jacques Delabrouille, Sanjit Mitra, Anthony Lewis, and Niels Oppermann for helpful discussions. We acknowledge the use of the Planck Legacy Archive (PLA). The development of Planck has been supported by ESA; CNES and CNRS/INSU-IN2P3-INP (France); ASI, CNR, and INAF (Italy); NASA and DOE (USA); STFC and UKSA (UK); CSIC, MICINN, and JA (Spain); Tekes, AoF, and CSC (Finland); DLR and MPG (Germany); CSA (Canada); DTU Space (Denmark); SER/SSO (Switzerland); RCN (Norway); SFI (Ireland); FCT/MCTES (Portugal); PRACE (EU). A description of the Planck Collaboration and a list of its members, including the technical or scientific activities in which they have been involved, can be found at http://www.sciops.esa.int/index.php?project=planck&page=Planck_Collaboration. We acknowledge the use of the Legacy Archive for Microwave Background Data Analysis (LAMBDA), part of the High Energy Astrophysics Science Archive Center (HEASARC). HEASARC/LAMBDA is a service of the Astrophysics Science Division at the NASA Goddard Space Flight Center. We also acknowledge the use of the EFFCONV [34], HEALPIX [35], CAMB [36], and COSMOMC packages [21].

[3]While WMAP does not scan along the ecliptic longitudes, the scan directions cover only about 30% of possible angles on the ecliptic equator, which are closer to being parallel to the ecliptic longitudes. As a result, the 41 GHz maps give $g_* < 0$, as the orientations of the 41 GHz beams are nearly parallel to WMAP's scan direction, whereas the 61 and 94 GHz maps give $g_* > 0$, as the orientations are nearly perpendicular to the scan direction [33]. This explanation is due to Ref. [31].

[4]http://irsa.ipac.caltech.edu/data/Planck/release_1/software.

[1] A. A. Starobinsky, Phys. Lett. B **91**, 99 (1980).
[2] K. Sato, Mon. Not. R. Astron. Soc. **195**, 467 (1981).
[3] A. H. Guth, Phys. Rev. D **23**, 347 (1981).
[4] A. D. Linde, Phys. Lett. **108B**, 389 (1982).
[5] A. Albrecht and P. J. Steinhardt, Phys. Rev. Lett. **48**, 1220 (1982).
[6] V. F. Mukhanov and G. Chibisov, JETP Lett. **33**, 532 (1981).
[7] G. Hinshaw *et al.*, Astrophys. J. Suppl. Ser. **208**, 19 (2013).
[8] P. Ade *et al.* (Planck Collaboration), arXiv:1303.5076.
[9] L. Ackerman, S. M. Carroll, and M. B. Wise, Phys. Rev. D **75**, 083502 (2007).
[10] J. Soda, Classical Quantum Gravity **29**, 083001 (2012).
[11] A. Maleknejad, M. Sheikh-Jabbari, and J. Soda, Phys. Rep. **528**, 161 (2013).
[12] E. Dimastrogiovanni, N. Bartolo, S. Matarrese, and A. Riotto, Adv. Astron. **2010**, 752670 (2010).
[13] N. Barnaby, R. Namba, and M. Peloso, Phys. Rev. D **85**, 123523 (2012).
[14] M. Shiraishi, E. Komatsu, M. Peloso, and N. Barnaby, J. Cosmol. Astropart. Phys. 05 (2013) 002.
[15] N. Bartolo, S. Matarrese, M. Peloso, and A. Ricciardone, Phys. Rev. D **87**, 023504 (2013).
[16] P. Ade *et al.* (Planck Collaboration), arXiv:1303.5084.
[17] F. Schmidt and L. Hui, Phys. Rev. Lett. **110**, 011301 (2013).
[18] N. Bartolo, S. Matarrese, M. Peloso, and A. Ricciardone, J. Cosmol. Astropart. Phys. 08 (2013) 022.
[19] Y.-Z. Ma, G. Efstathiou, and A. Challinor, Phys. Rev. D **83**, 083005 (2011).
[20] D. Hanson and A. Lewis, Phys. Rev. D **80**, 063004 (2009).
[21] A. Lewis and S. Bridle, Phys. Rev. D **66**, 103511 (2002).
[22] A. R. Pullen and M. Kamionkowski, Phys. Rev. D **76**, 103529 (2007).
[23] P. Ade *et al.* (Planck Collaboration), arXiv:1303.5062.
[24] N. Aghanim *et al.* (Planck Collaboration), arXiv:1303.5063.
[25] P. Ade *et al.* (Planck Collaboration), arXiv:1303.5067.
[26] P. Ade *et al.* (Planck Collaboration), arXiv:1303.5072.
[27] N. Aghanim *et al.* (Planck Collaboration), arXiv:1303.5065.
[28] P. Ade *et al.* (Planck Collaboration), arXiv:1303.5068.
[29] N. E. Groeneboom and H. K. Eriksen, Astrophys. J. **690**, 1807 (2009).
[30] N. E. Groeneboom, L. Ackerman, I. K. Wehus, and H. K. Eriksen, Astrophys. J. **722**, 452 (2010).
[31] D. Hanson, A. Lewis, and A. Challinor, Phys. Rev. D **81**, 103003 (2010).
[32] C. L. Bennett *et al.*, Astrophys. J. Suppl. Ser. **208**, 20 (2013).
[33] R. Hill *et al.* (WMAP Collaboration), Astrophys. J. Suppl. Ser. **180**, 246 (2009).
[34] S. Mitra, G. Rocha, K. M. Górski, K. M. Huffenberger, H. K. Eriksen, M. A. J. Ashdown, and C. R. Lawrence, Astrophys. J. Suppl. Ser. **193**, 5 (2011).
[35] K. M. Gorski, E. Hivon, A. J. Banday, B. D. Wandelt, F. K. Hansen, M. Reinecke, and M. Bartelman, Astrophys. J. **622**, 759 (2005).
[36] A. Lewis, A. Challinor, and A. Lasenby, Astrophys. J. **538**, 473 (2000).